MIMO Radar Space–Time Adaptive Processing Using Prolate Spheroidal Wave Functions

Chun-Yang Chen, *Student Member, IEEE*, and P. P. Vaidyanathan, *Fellow, IEEE*

***Abstract*—In the traditional transmitting beamforming radar system, the transmitting antennas send coherent waveforms which form a highly focused beam. In the multiple-input multiple-output (MIMO) radar system, the transmitter sends noncoherent (possibly orthogonal) broad (possibly omnidirectional) waveforms. These waveforms can be extracted at the receiver by a matched filterbank. The extracted signals can be used to obtain more diversity or to improve the spatial resolution for clutter. This paper focuses on space–time adaptive processing (STAP) for MIMO radar systems which improves the spatial resolution for clutter. With a slight modification, STAP methods developed originally for the single-input multiple-output (SIMO) radar (conventional radar) can also be used in MIMO radar. However, in the MIMO radar, the rank of the jammer-and-clutter subspace becomes very large, especially the jammer subspace. It affects both the complexity and the convergence of the STAP algorithm. In this paper, the clutter space and its rank in the MIMO radar are explored. By using the geometry of the problem rather than data, the clutter subspace can be represented using prolate spheroidal wave functions (PSWF). A new STAP algorithm is also proposed. It computes the clutter space using the PSWF and utilizes the block-diagonal property of the jammer covariance matrix. Because of fully utilizing the geometry and the structure of the covariance matrix, the method has very good SINR performance and low computational complexity.**

***Index Terms*—Clutter subspaces, multiple-input multiple-output (MIMO) radar, prolate spheroidal wave function, space–time adaptive processing (STAP).**

I. Introduction

RECENTLY, the concept of multiple-input multiple-output (MIMO) radars has drawn considerable attention [1]–[13]. MIMO radars emit orthogonal waveforms [1]–[10] or noncoherent [11]–[13] waveforms instead of transmitting coherent waveforms which form a focused beam in traditional transmitter based beamforming. In the MIMO radar receiver, a matched filterbank is used to extract the orthogonal waveform components. There are two different kinds of approaches for using the noncoherent waveforms. First, increased spatial diversity can be obtained [4], [5]. In this scenario, the transmitting antenna elements are far enough from each other compared to the distance from the target. Therefore, the target radar cross sections (RCS) are independent random variables for different transmitting paths. When the orthogonal components are transmitted from different antennas, each orthogonal waveform will carry independent information about the target. This spatial diversity can be utilized to perform better detection [4], [5]. Second, a better spatial resolution for clutter can be obtained. In this scenario, the distances between transmitting antennas are small enough compared to the distance between the target and the radar station. Therefore, the target RCS is identical for all transmitting paths. The phase differences caused by different transmitting antennas along with the phase differences caused by different receiving antennas can form a new *virtual array* steering vector. With judiciously designed antenna positions, one can create a very long array steering vector with a small number of antennas. Thus, the spatial resolution for clutter can be dramatically increased at a small cost [1], [2]. In this paper, we focus on this second advantage.

The adaptive techniques for processing the data from airborne antenna arrays are called space–time adaptive processing (STAP) techniques. The basic theory of STAP for the traditional single-input multiple-output (SIMO) radar has been well developed [32], [33]. There have been many algorithms proposed in [27]–[33] and the references therein for improving the complexity and convergence of the STAP in the SIMO radar. With a slight modification, these methods can also be applied to the MIMO radar case. The MIMO extension of STAP can be found in [2]. The MIMO radar STAP for multipath clutter mitigation can be found in [10]. However, in the MIMO radar, the STAP becomes even more challenging because of the extra dimension created by the orthogonal waveforms. On one hand, the extra dimension increases the rank of the jammer and clutter subspace, especially the jammer subspace. This makes the STAP more complex. On the other hand, the extra degrees of freedom created by the MIMO radar allows us to filter out more clutter subspace with little effect on signal-to-interference-plus-noise ratio (SINR).

In this paper, we explore the clutter subspace and its rank in MIMO radar. Using the geometry of the MIMO radar and the prolate spheroidal wave function (PSWF), a method for computing the clutter subspace is developed. Then we develop a STAP algorithm which computes the clutter subspace using the geometry of the problem rather than data and utilizes the block-diagonal structure of the jammer covariance matrix. Because of fully utilizing the geometry and the structure of the covariance matrix, our method has very good SINR performance and significantly lower computational complexity compared to fully adaptive methods (Section V-B).

In practice, the clutter subspace might change because of effects such as the internal clutter motion (ICM), velocity misalignment, array manifold mismatch, and channel mismatch [32]. In this paper, we consider an "ideal model," which does

Manuscript received November 15, 2006; revised July 22, 2007. The associate editor coordinating the review of this manuscript and approving it for publication was Prof. Steven M. Kay. This work was supported in part by the ONR Grant N00014-06-1-0011 and the California Institute of Technology.

The authors are with the Electrical Engineering Department, California Institute of Technology, Pasadena, CA 91125 USA (e-mail: cyc@caltech.edu;ppvnath@systems.caltech.edu).

Digital Object Identifier 10.1109/TSP.2007.907917

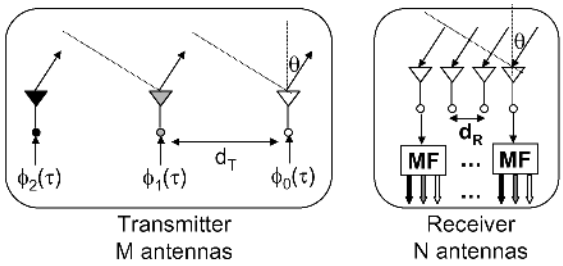

Fig. 1. Illustration of a MIMO radar system with $M = 3$ and $N = 4$.

not take these effects into account. When this model is not valid, the performance of the algorithm will degrade. One way to overcome this might be to estimate the clutter subspace by using a combination of both the assumed geometry and the received data. Another way might be to develop a more robust algorithm against the clutter subspace mismatch. These ideas will be explored in the future.

The rest of the paper is organized as follows. In Section II, the concept of MIMO radar will be briefly reviewed. In Section III, we formulate the STAP approach for MIMO radar. In Section IV, we explore the clutter subspace and its rank in the MIMO radar. Using PSWF, we construct a data-independent basis for clutter signals. In Section V, we propose a new STAP method for MIMO radar. This method utilizes the technique proposed in Section IV to find the clutter subspace and estimates the jammer-plus-noise covariance matrix separately. Finally, the beamformer is calculated by using matrix inversion lemma. As we will see later, this method has very satisfactory SINR performance. In Section VI, we compare the SINR performance of different STAP methods based on numerical simulations. Finally, Section VII concludes the paper.

Notations. Matrices are denoted by capital letters in boldface (e.g., $\mathbf{A}$). Vectors are denoted by lowercase letters in boldface (e.g., $\mathbf{x}$). Superscript † denotes transpose conjugation. The notation $\mathrm{diag}(\mathbf{A}, \mathbf{A}, \ldots, \mathbf{A})$ denotes a block-diagonal matrix whose diagonal blocks are $\mathbf{A}$. The notation $\lceil a \rceil$ is defined as the smallestinteger larger than a.

II. Review of the MIMO Radar

In this section, we briefly review the MIMO radar idea. More detailed reviews can be found in [1], [2], [6]. We will focus on using MIMO radar to increase the degrees of freedom. Fig. 1 illustrates a MIMO radar system. The transmitting antennas emit orthogonal waveforms $\phi_k(\tau)$. At each receiving antenna, these orthogonal waveforms can be extracted by M matched filters, where M is the number of transmitting antennas. Therefore, there are a total of NM extracted signals, where N is the number of receiving antennas. The signals reflected by the target at direction θ can be expressed as

$$\rho_t e^{j\frac{2\pi}{\lambda}(nd_R \sin\theta + md_T \sin\theta)} \tag{1}$$

for $n = 0, 1, \cdots, N-1$, $m = 0, 1, \cdots, M-1$. Here ρ_t is the amplitude of the signal reflected by the target, d_R is the spacing between the receiving antennas, and d_T is the spacing between the transmit antennas. The phase differences are created by both transmitting and receiving antenna locations. Define $f_s \triangleq (d_R/\lambda)\sin\theta$ and $\gamma \triangleq d_T/d_R$. Equation (1) can be further simplified as

$$\rho_t e^{j2\pi f_s(n+\gamma m)}.$$

If we choose $\gamma = N$, the set $\{n+\gamma m\} = \{0, 1, \cdots, NM-1\}$. Thus, the NM signals in (1) can be viewed as the signals received by a *virtual array* with NM elements [2], as shown in Fig. 2. It is as if we have a receiving array of NM elements. Thus, NM degrees of freedom can be obtained with only $N+M$ physical array elements. One can view the antenna array as a way to sample the electromagnetic wave in the spatial domain. The MIMO radar idea allows "sampling" in both transmitter and receiver and creates a total of NM "samples." Taking advantage of these extra samples in spatial domain, a better spatial resolution can be obtained.

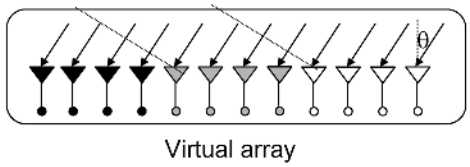

Fig. 2. Virtual array corresponding to the MIMO radar in Fig. 1.

III. STAP in MIMO Radar

In this section, we formulate the STAP problem in MIMO radar. The MIMO extension for STAP first appeared in [2]. We will focus on the idea of using the extra degrees of freedom to increase the spatial resolution for clutter.

A. Signal Model

Fig. 3 shows the geometry of the MIMO radar STAP with uniform linear arrays (ULAs), where:

1) d_T is the spacing of the transmitting antennas;
2) d_R is the spacing of the receiver antennas;
3) M is the number of transmitting antennas;
4) N is the number of the receiving antennas;
5) T is the radar pulse period;
6) l indicates the index of radar pulse (slow time);
7) τ represents the time within the pulse (fast time);
8) v_t is the target speed toward the radar station;
9) v is the speed of the radar station.

Notice that the model assumes the two antenna arrays are linear and parallel. The transmitter and the receiver are close enough so that they share the same angle variable θ. The radar station movement is assumed to be parallel to the linear antenna array. This assumption has been made in most of the airborne ground moving target indicator (GMTI) systems. Each array is composed of omnidirectional elements. The transmitted signals of the mth antenna can be expressed as

$$x_m(lT+\tau) = \sqrt{E}\phi_m(\tau)e^{j2\pi f(lT+\tau)}$$

for $m = 1, 2, \ldots, M-1$, where $\phi_m(\tau)$ is the baseband pulse waveform, f is the carrier frequency, and E is the transmitted

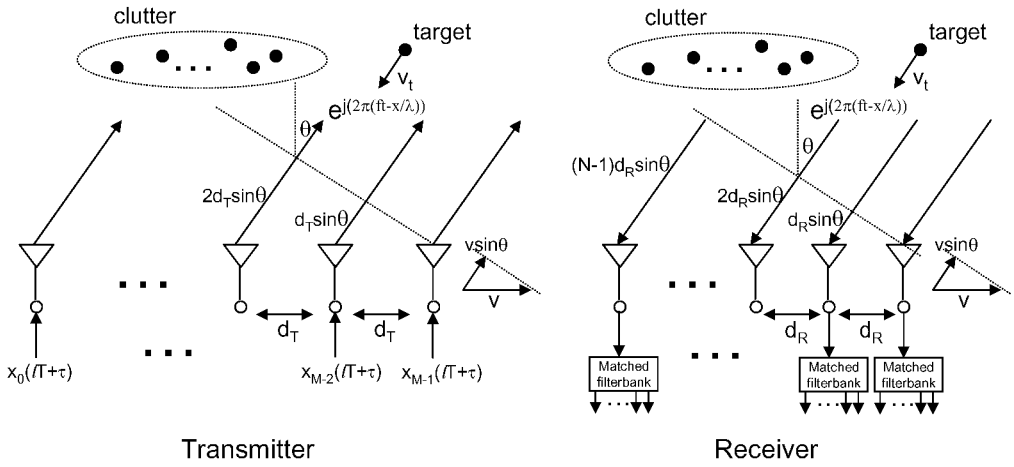

Fig. 3. This illustrates a MIMO radar system with M transmitting antennas and N receiving antennas. The radar station is moving with speed v.

energy for the pulse. The demodulated received signal of the nth antenna can be expressed as

$$\begin{aligned} & y_n\left(lT+\tau+\frac{2r}{c}\right) \\ & \quad \approx \sum_{m=0}^{M-1} \rho_t \phi_m(\tau) e^{j\frac{2\pi}{\lambda}(\sin\theta_t(2vTl+d_R n+d_T m)+2v_t Tl)} \\ & \qquad + \sum_{i=0}^{N_c-1}\sum_{m=0}^{M-1} \rho_i \phi_m(\tau) e^{j\frac{2\pi}{\lambda}(\sin\theta_i(2vTl+d_R n+d_T m))} \\ & \qquad + y_n^{(J)}(lT+\tau+\frac{2r}{c}) + y_n^{(w)}(lT+\tau+\frac{2r}{c}) \end{aligned} \tag{2}$$

where:

1) r is the distance of the range bin of interest;
2) c is the speed of light;
3) ρ_t is the amplitude of the signal reflected by the target;
4) ρ_i is the amplitude of the signal reflected by the ith clutter;
5) θ_t is the looking direction of the target;
6) θ_i is the looking direction of the ith clutter;
7) N_c is the number of clutter signals;
8) $y_n^{(J)}$ is the jammer signal in the nth antenna output;
9) $y_n^{(w)}$ is the white noise in the nth antenna output.

For convenience, all of the parameters used in the signal model are summarized in Table I. The first term in (2) represents the signal reflected by the target. The second term is the signal reflected by the clutter. The last two terms represent the jammer signal and white noise. We assume there is no ICM or antenna array misalignment [32]. The phase differences in the reflected signals are caused by the Doppler shift, the differences of the receiving antenna locations, and the differences of the transmitting antenna locations. In the MIMO radar, the transmitting waveforms $\phi_m(\tau)$ satisfy orthogonality:

$$\int \phi_m(\tau)\phi_k^*(\tau)d\tau = \delta_{mk}. \tag{3}$$

TABLE I
LIST OF THE PARAMETERS USED IN THE SIGNAL MODEL

d_T	spacing of the transmitting antennas
d_R	spacing of the receiving antennas
M	number of the transmitting antennas
N	number of the receiving antennas
T	radar pulse period
l	index of radar pulse (slow time)
τ	time within the pulse (fast time)
v_t	target speed toward the radar station
x_m	transmitted signal in the mth antenna
ϕ_m	baseband pulse waveforms
y_n	demodulated received signal in the nth antenna
v_t	target speed toward the radar station
v	speed of the radar station
r	distance of the range bin of interest
c	speed of light
ρ_t	amplitude of the signal reflected by the target
ρ_i	amplitude of the signal reflected by the ith clutter
θ_t	looking direction of the target
θ_i	looking direction of the ith clutter
N_c	number of clutter signals
$y_n^{(J)}$	jammer signal in the nth antenna output
$y_n^{(w)}$	white noise in the nth antenna output

The sufficient statistics can be extracted by a bank of matched filters as shown in Fig. 3. The extracted signals can be expressed as

$$\begin{aligned} y_{n,m,l} &\triangleq \int y_n(lT+\tau+\frac{2r}{c})\phi_m^*(\tau)d\tau \\ &= \rho_t e^{j\frac{2\pi}{\lambda}(\sin\theta_t(2vTl+d_R n+d_T m)+2v_t Tl)} \\ &\quad + \sum_{i=0}^{N_c-1} \rho_i e^{j\frac{2\pi}{\lambda}(\sin\theta_i(2vTl+d_R n+d_T m))} \\ &\quad + y_{n,m,l}^{(J)} + y_{n,m,l}^{(w)} \end{aligned} \tag{4}$$

for $n = 0,1,\ldots,N-1, m = 0,1,\ldots,M-1$, and $l = 0,1,\ldots,L-1$, where $y_{n,m,l}^{(J)}$ is the corresponding jammer signal, $y_{n,m,l}^{(w)}$ is the corresponding white noise, and L is the number of the pulses in a coherent processing interval (CPI).

To simplify the above equation, we define the following normalized spatial and Doppler frequencies:

$$f_s \triangleq \frac{d_R}{\lambda}\sin\theta_t, f_{s,i} \triangleq \frac{d_R}{\lambda}\sin\theta_i$$
$$f_D \triangleq \frac{2(v\sin\theta_t + v_t)}{\lambda}T. \tag{5}$$

One can observe that the normalized Doppler frequency of the target is a function of both target looking direction and speed. Throughout this paper we shall make the assumption $d_R = \lambda/2$ so that spatial aliasing is avoided. Using the above definition, we can rewrite the extracted signal in (4) as

$$y_{n,m,l} = \rho_t e^{j2\pi f_s(n+\gamma m)} e^{j2\pi f_D l} + \sum_{i=0}^{Nc-1} \rho_i e^{j2\pi f_{s,i}(n+\gamma m+\beta l)} + y_{n,m,l}^{(J)} + y_{n,m,l}^{(w)} \tag{6}$$

for $n = 0,1,\ldots,N-1, m = 0,1,\ldots,M-1$, and $l = 0,1,\ldots,L-1$, where

$$\gamma \triangleq d_T/d_R \text{ and } \beta \triangleq 2vT/d_R. \tag{7}$$

B. Fully Adaptive MIMO-STAP

The goal of space–time adaptive processing (STAP) is to find a linear combination of the extracted signals so that the SINR can be maximized. Thus, the target signal can be extracted from the interferences, clutter, and noise to perform the detection. Stacking the MIMO STAP signals in (6), we obtain the NML vector

$$\mathbf{y} = (y_{0,0,0} \quad y_{1,0,0}\cdots y_{N-1,M-1,L-1})^T. \tag{8}$$

Then, the linear combination can be expressed as $\mathbf{w}^\dagger\mathbf{y}$, where $\mathbf{w}$ is the weight vector for the linear combination. The SINR maximization can be obtained by minimizing the total variance under the constraint that the target response is unity. It can be expressed as the following optimization problem:

$$\min_{\mathbf{w}} \mathbf{w}^\dagger\mathbf{R}\mathbf{w}$$
$$\text{subject to } \mathbf{w}^\dagger\mathbf{s}(f_s,f_D) = 1 \tag{9}$$

where $\mathbf{R} \triangleq E[\mathbf{y}\mathbf{y}^\dagger]$, and $\mathbf{s}(f_s,f_D)$ is the size-NML MIMO space–time steering vector, which consists of the elements

$$e^{j2\pi f_s(n+\gamma m)}e^{j2\pi f_D l} \tag{10}$$

for $n = 0,1,\ldots,N-1, m = 0,1,\ldots,M-1$, and $l = 0,1,\ldots,L-1$. This $\mathbf{w}$ is called minimum variance distortionless response (MVDR) beamformer [20]. The covariance matrix $\mathbf{R}$ can be estimated by using the neighboring range bin cells. In practice, in order to prevent self-nulling, a target-free covariance matrix can be estimated by using guard cells [32]. The well-known solution to the above problem is [20]

$$\mathbf{w} = \frac{\mathbf{R}^{-1}\mathbf{s}(f_s,f_D)}{\mathbf{s}(f_s,f_D)^\dagger\mathbf{R}^{-1}\mathbf{s}(f_s,f_D)}. \tag{11}$$

However, the covariance matrix $\mathbf{R}$ is $NML\times NML$. It is much larger than in the SIMO case because of the extra dimension. The complexity of the inversion of such a large matrix is high. The estimation of such a large covariance matrix also converges slowly. To overcome these problems, partially adaptive techniques can be applied. The methods described in Section VI are examples of such partially adaptive techniques. In SIMO radar literature such partially adaptive methods are commonly used [32], [33].

C. Comparison With SIMO System

In the traditional transmit beamforming, or SIMO radar, the transmitted waveforms are coherent and can be expressed as

$$\phi_m(\tau) = \phi(\tau)w_{Tm}$$

for $m = 1,2,\ldots,M-1$, where $\{w_{Tm}\}$ are the transmit beamforming weights. The sufficient statistics can be extracted by a single matched filter for every receiving antenna. The extracted signal can be expressed as

$$\begin{aligned} y_{n,l} &\triangleq \int y_n(lT+\tau+\frac{2r}{c})\phi^*(\tau)d\tau \\ &= \rho_t e^{j2\pi f_s n}e^{j2\pi f_D l}\sum_{m=0}^{M-1} w_{Tm}e^{j2\pi f_s\gamma m} \\ &\quad + \sum_{i=0}^{N_c-1}\rho_i e^{j2\pi f_{s,i}(n+\beta l)}\sum_{m=0}^{M-1} w_{Tm}e^{j2\pi f_{s,i}\gamma m} \\ &\quad + y_{n,l}^J + y_{n,l}^{(w)}, \end{aligned} \tag{12}$$

for $n = 0,1,\ldots,N-1$, and $l = 0,1,\ldots,L-1$, where $y_{n,l}^{(J)}$ is the corresponding jammer signal, and $y_{n,l}^{(w)}$ is the corresponding white noise. Comparing the MIMO signals in (6) and the SIMO signals in (12), one can see that a linear combination with respect to m has been performed on the SIMO signal in the target term and the clutter term. The MIMO radar, however, leaves all degrees of freedom to the receiver. Note that in the receiver, one can perform the same linear combination with respect to m on the MIMO signal in (6) to create the SIMO signal in (12). The only difference is that the transmitting power for the SIMO signal is less because of the focused beam used in the transmitter. For the SIMO radar, the number of degrees of freedom is M in the transmitter and NL in the receiver. The total number of degrees of freedom is $M+NL$. However, for the MIMO radar, the number of degrees of freedom is NML which is much larger than $M+NL$. These extra degrees of freedom can be used to obtain a better spatial resolution for clutter.

The MIMO radar transmits omnidirectional orthogonal waveforms from each antenna element. Therefore, it illuminates all angles. The benefit of SIMO radar is that it transmits focused beams which saves transmitting power. Therefore, for a particular angle of interest, the SIMO radar enjoys a processing gain of M compared to the MIMO radar. However, for some applications like scanning or imaging, it is necessary to illuminate all angles. In this case, the benefit of a focused beam no longer exists because both systems need to consume the same energy for illuminating all angles. The SIMO system will need to steer the focused transmit beam to illuminate all angles.

A second point is that for the computation of the MIMO beamformer in (11), the matrix inversion $\mathbf{R}^{-1}$ needs to be computed only once and it can be applied for all angles. The transmitting array in a MIMO radar does not have a focused beam. So, all the ground points within a range bin are uniformly illuminated. The clutter covariance seen by the receiving-antenna array is, therefore, the same for all angles. In the SIMO case, the matrix inversions need to be computed for different angles because the clutter signal changes as the beam is steered through all angles.

D. Virtual Array

Observing the MIMO space–time steering vector defined in (10), one can view the first term $e^{j2\pi f_s(n+\gamma m)}$ as a sampled version of the sinusoidal function $e^{j2\pi f_s x}$. Recall that γ is defined in (6) as the ratio of the antenna spacing of the transmitter and receiver. To obtain a good spatial frequency resolution, these signals should be critically sampled and have long enough duration. One can choose $\gamma = N$ because it maximizes the time duration while maintaining critical sampling [2], as shown in Fig. 2. Sorting the sample points $n+\gamma m$ for $n = 0, 1, \ldots, N-1$, and $m = 0, 1, \ldots, M-1$, we obtain the sorted sample points $k = 0, 1, \ldots, NM-1$. Thus, the target response in (10) can be rewritten as

$$e^{j2\pi f_s k} e^{j2\pi f_D l}$$

for $k = 0, 1, \ldots, NM-1$, and $l = 0, 1, \ldots, L-1$. It is as if we have a virtual receiving array with NM antennas. However, the resolution is actually obtained by only M antennas in the transmitter and N antennas in the receiver. Fig. 4 compares the SINR performance of the MIMO system and the SIMO system in the array looking direction of zero degree, that is, $f_s = 0$. The optimal space–time beamformer described in (11) is used. The parameter L equals 16, and β equals 1.5 in this example. In all plots, it is assumed that the energy transmitted by any single antenna element to illuminate all angles is fixed. The SINR drops near zero Doppler frequency because it is not easy to distinguish the slowly moving target from the still ground clutter. The MIMO system with $\gamma = 1$ has a slightly better performance than the SIMO system with the same antenna structure. For the virtual array structure where $\gamma = N$, the MIMO system has a very good SINR performance, and it is close to the performance of the SIMO system with NM antennas because they have the same resolution for the target signal and the clutter signals. The small difference comes from the fact that the SIMO system with NM antennas has a better spatial resolution for the jammer signals. This example shows that the choice of γ is very crucial in the MIMO radar. With the choice $\gamma = 10 = N$, the MIMO radar with only 15 antenna elements has about the same performance as the SIMO radar with 51 array elements. This example also shows that the MIMO radar system has a much better spatial resolution for clutter compared to the traditional SIMO system with same number of physical antenna elements.

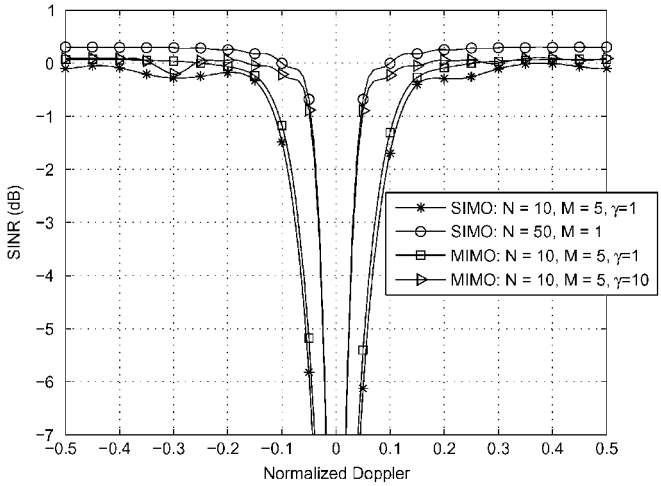

Fig. 4. SINR at looking direction zero as a function of the Doppler frequencies for different SIMO and MIMO systems.

IV. Clutter Subspace in MIMO Radar

In this section, we explore the clutter subspace and its rank in the MIMO radar system. The covariance matrix $\mathbf{R}$ in (9) can be expressed as $\mathbf{R} = \mathbf{R}_t + \mathbf{R}_c + \mathbf{R}_J + \sigma^2\mathbf{I}$, where $\mathbf{R}_t$ is the covariance matrix of the target signal, $\mathbf{R}_c$ is the covariance matrix of the clutter, $\mathbf{R}_J$ is the covariance matrix of the jammer, and σ^2 is the variance of the white noise. The clutter subspace is defined as the range space of $\mathbf{R}_c$ and the clutter rank is defined as the rank of $\mathbf{R}_c$. In the space–time adaptive processing (STAP) literature, it is a well-known fact that the clutter subspace usually has a small rank. It was first pointed out by Klemm in [18], that the clutter rank is approximately $N + L$, where N is the number of receiving antennas and L is the number of pulses in a coherent processing interval (CPI). In [16] and [17], a rule for estimating the clutter rank was proposed. The estimated rank is approximately

$$N + \beta(L-1) \tag{13}$$

where $\beta = 2vT/d_R$. This is called Brennan's rule. In [15], this rule has been extended to the case with arbitrary arrays. Taking advantage of the low rank property, the STAP can be performed in a lower dimensional space so that the complexity and the convergence can be significantly improved [26]–[33]. This result will now be extended to the MIMO radar. These techniques are often called *partially adaptive methods* or *subspace methods*.

A. Clutter Rank in MIMO Radar

We first study the clutter term in (6) which is expressed as

$$y_{n,m,l}^{(c)} = \sum_{i=0}^{Nc-1} \rho_i e^{j2\pi f_{s,i}(n+\gamma m+\beta l)}$$

for $n = 0, 1, \ldots, N-1, m = 0, 1, \ldots, M-1$, and $l = 0, 1, \ldots, L-1$. Note that $-0.5 < f_{s,i} < 0.5$ because $d_R = \lambda/2$. Define $c_{i,n,m,l} = e^{j2\pi f_{s,i}(n+\gamma m+\beta l)}$ and

$$\mathbf{c}_i = (c_{i,0,0,0}, c_{i,1,0,0}, \ldots, c_{i,N-1,M-1,L-1})^T. \quad (14)$$

By stacking the signals $\left\{y_{n,m,l}^{(c)}\right\}$ into a vector, one can obtain

$$\mathbf{y}^{(c)} = \sum_{i=0}^{N_c-1} \rho_i \mathbf{c}_i.$$

Assume that ρ_i are zero-mean independent random variables with variance $\sigma_{c,i}^2$. The clutter covariance matrix can be expressed as

$$\mathbf{R}_c = E\left[\mathbf{y}^{(c)}\mathbf{y}^{(c)\dagger}\right] = \sum_{i=0}^{N_c-1} \sigma_{c,i}^2 \mathbf{c}_i \mathbf{c}_i^\dagger.$$

Therefore, $\text{span}(\mathbf{R}_c) = \text{span}(\mathbf{C})$, where

$$\mathbf{C} \triangleq (\mathbf{c}_0, \mathbf{c}_1, \ldots, \mathbf{c}_{N_c-1}).$$

The vector $\mathbf{c}_i$ consists of the samples of $e^{j2\pi f_{s,i}x}$ at points $\{n+\gamma m+\beta l\}$, where γ and β are defined in (7). In general, $\mathbf{c}_i$ is a *nonuniformly* sampled version of the band-limited sinusoidal waveform $e^{j2\pi f_{s,i}x}$. If γ and β are both integers, the sampled points $\{n+\gamma m+\beta l\}$ can only be integers in

$$\{0, 1, \ldots, N+\gamma(M-1)+\beta(L-1)\}.$$

If $N+\gamma(M-1)+\beta(L-1) \le NML$, there will be repetitions in the sample points. In other words, some of the row vectors in $\mathbf{C}$ will be exactly the same and there will be at most $N+\gamma(M-1)+\beta(L-1)$ distinct row vectors in $\mathbf{C}$. Therefore, the rank of $\mathbf{C}$ is less than $N+\gamma(M-1)+\beta(L-1)$. So is the rank of $\mathbf{R}_c$. We summarize this fact as the following

Theorem 1: If γ and β are both integers, then rank $(\mathbf{R}_c) \le \min(N+\gamma(M-1)+\beta(L-1), N_c, NML)$. ■

Usually N_c and NML are much larger than $N+\gamma(M-1)+\beta(L-1)$. Therefore, $N+\gamma(M-1)+\beta(L-1)$ is a good estimation of the clutter rank. This result can be viewed as an extension of Brennan's rule [16], given in (13), to the MIMO radar case.

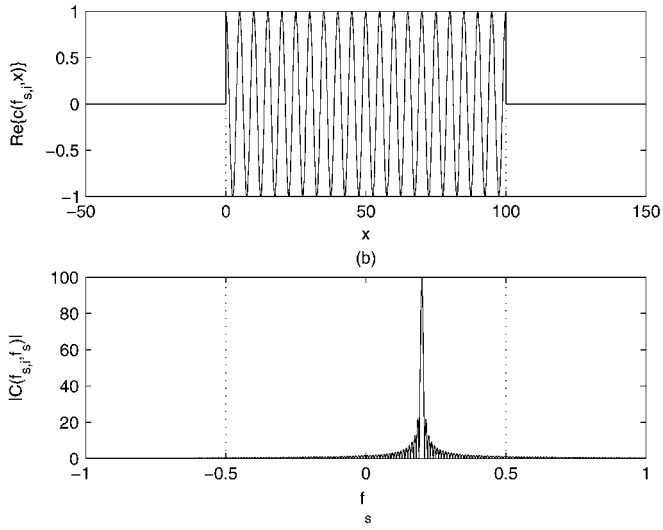

Fig. 5. Example of the signal $c(x; f_{s,i})$. (a) Real part. (b) Magnitude response of Fourier transform.

Now, we focus on the general case where γ and β are real numbers. The vector $\mathbf{c}_i$ in (14) can be viewed as a nonuniformly sampled version of the truncated sinusoidal function

$$c(x; f_{s,i}) \triangleq \begin{cases} e^{j2\pi f_{s,i}x}, & 0 \le x \le X \\ 0, & \text{otherwise} \end{cases} \quad (15).$$

where $X \triangleq N-1+\gamma(M-1)+\beta(L-1)$. Furthermore, $-0.5 \le f_{s,i} \le 0.5$ because d_R is often selected as $\lambda/2$ in (5) to avoid aliasing. Therefore, the energy of these signals is mostly confined to a certain time-frequency region. Fig. 5 shows an example of such a signal. Such signals can be well approximated by linear combinations of $\lceil 2WX+1 \rceil$ orthogonal functions [19], where W is the one-sided bandwidth and X is the duration of the time-limited functions. In the next section, more details on this will be discussed using PSWF. In this case, we have $W = 0.5$ and $2WX+1 = N+\gamma(M-1)+\beta(L-1)$. The vectors $\mathbf{c}_i$ can be also approximated by a linear combination of the nonuniformly sampled versions of these $\lceil N+\gamma(M-1)+\beta(L-1) \rceil$ orthogonal functions. Thus, in the case where γ and β are nonintegers, we can conclude that only $\lceil N+\gamma(M-1)+\beta(L-1) \rceil$ eigenvalues of the matrix $\mathbf{R}_c$ are significant. In other words

$$\text{rank}(\mathbf{R}_c) \approx \lceil N+\gamma(M-1)+\beta(L-1) \rceil. \quad (16)$$

Note that the definition of this approximate rank is actually the number of the dominant eigenvalues. This notation has been widely used in the STAP literature [32], [33]. In the SIMO radar case, using Brennan's rule, the ratio of the clutter rank and the total dimension of the space–time steering vector can be approximated as

$$\frac{N+\beta(L-1)}{NL} = \frac{1}{L} + \frac{\beta(L-1)}{NL}.$$

In the MIMO radar case with $\gamma = N$, the corresponding ratio becomes

$$\frac{N + N(M-1) + \beta(L-1)}{NML} = \frac{1}{L} + \frac{\beta(L-1)}{NML}.$$

One can observe that the clutter rank now becomes a smaller portion of the total dimension because of the extra dimension introduced by the MIMO radar. *Thus the MIMO radar receiver can null out the clutter subspace with little effect on SINR*. Therefore, a better spatial resolution for clutter can be obtained.

The result can be further generalized for the array with arbitrary linear antenna deployment. Let $x_{T,m}, m = 0, 1, \ldots, M-1$ be the transmitting antenna locations, $x_{R,n}, n = 0, 1, \ldots, N-1$ be the receiving antenna locations, and v be the speed of the radar station. Without loss of generality, we set $x_{T,0} = 0$ and $x_{R,0} = 0$. Then the clutter signals can be expressed as

$$y^{(c)}_{n,m,l} = \sum_{i=0}^{N_c-1} \rho_i e^{j\frac{2\pi}{\lambda}\sin\theta_i((x_{R,n}+x_{T,m}+2vTl))}$$

for $n = 0, 1, \ldots, N-1, m = 0, 1, \ldots, M-1$, and $l = 0, 1, \ldots, L-1$, where θ_i is the looking-direction of the ith clutter. The term

$$e^{j\frac{2\pi}{\lambda}\sin\theta_i(x_{R,n}+x_{T,m}+2vTl)}$$

can also be viewed as a nonuniform sampled version of the function $e^{j\frac{2\pi}{\lambda}\sin\theta_i x}$. Using the same argument we have made in the ULA case, one can obtain

$$\text{rank}(\mathbf{R}_c) \approx \lceil 1 + \frac{2}{\lambda}(x_{R,N-1} + x_{T,M-1} + 2vT(L-1))\rceil.$$

The quantity $x_{R,N-1} + x_{T,M-1} + 2vT(L-1)$ can be regarded as the total aperture of the space–time virtual array. One can see that the number of dominant eigenvalues is proportional to the ratio of the total aperture of the space–time virtual array and the wavelength.

B. Data-Independent Estimation of the Clutter Subspace With PSWF

The clutter rank can be estimated by using (16) and the parameters N, M, L, β, and γ. However, the clutter subspace is often estimated by using data samples instead of using these parameters [26]–[33]. In this section, we propose a method which estimates the clutter subspace using the geometry of the problem rather than the received signal. The main advantage of this method is that it is data independent. The clutter subspace obtained by this method can be used to improve the convergence of the STAP. Experiments also show that the estimated subspace is very accurate in the ideal case (without ICM and array misalignment).

In Fig. 5, one can see that the signal in (15) is time-limited and most of its energy is concentrated on $-0.5 \le f_s \le 0.5$. To approximate the subspace that contains such signals, we find the basis functions which are time-limited and concentrate their energy on the corresponding bandwidth. Such basis functions are the solutions of the following integral equation [19]:

$$\mu\psi(x) = \int_0^X \text{sinc}(2W(x-\zeta))\psi(\zeta)d\zeta$$

where $\text{sinc}(x) \triangleq \frac{\sin\pi x}{\pi x}$ and μ is a scalar to be solved. This integral equation has infinite number of solutions $\psi_i(x)$ and μ_i for $i = 0, 1, \ldots, \infty$. The solution $\psi_i(x)$ is called PSWF. By the maximum principle [36], the solution satisfies

$$\begin{aligned}
&\psi_0(x) \\
&\quad = \arg\max_{\|\psi\|=1} \int_0^X \int_0^X \psi^*(x)\text{sinc}(2W(x-\zeta))\psi(\zeta)d\zeta dx \\
&\psi_i(x) \\
&\quad = \arg\max_{\|\psi\|=1} \int_0^X \int_0^X \psi^*(x)\text{sinc}(2W(x-\zeta))\psi(\zeta)d\zeta dx \\
&\text{subject to} \int_0^X \psi(x)\psi_k^*(x)dx \\
&\quad = 0, \text{for } k = 0, 1, \ldots, i-1
\end{aligned}$$

for $i = 1, 2, \ldots, \infty$. The function $\psi_i(x)$ is orthogonal to the previous basis components $\psi_k(x)$, for $k < i$ while concentrating most of its energy on the bandwidth $[-W, W]$. Moreover, only the first $\lceil 2WX + 1\rceil$ eigenvalues μ_i are significant [19]. Therefore, the time-band-limited function $c(x; f_{s,i})$ in (15) can be well approximated by linear combinations of $\psi_i(x)$ for $i = 0, 1, \ldots, \lceil 2WX + 1\rceil$. In this case, $W = 0.5$ and $2WX + 1 = N + \gamma(M-1) + \beta(L-1)$. Thus, the nonuniformly sampled versions of $c(x; f_{s,i})$, namely $c_{i,n,m,l}$, can be approximated by the linear combination

$$c_{i,n,m,l} \triangleq e^{j2\pi f_{s,i}(n+\gamma m+\beta l)} \approx \sum_{k=0}^{r_c-1} \alpha_{i,k}\psi_k(n + \gamma m + \beta l),$$

for some $\{\alpha_{i,k}\}$, where

$$r_c \triangleq \lceil N + \gamma(M-1) + \beta(L-1)\rceil. \tag{17}$$

Stacking the above elements into vectors, we have

$$\mathbf{c}_i \approx \sum_{k=0}^{r_c-1} \alpha_{i,k}\mathbf{u}_k$$

where $\mathbf{u}_k$ is a vector that consists of the elements $\psi_k(n + \gamma m + \beta l)$. Finally, we have

$$\text{span}(\mathbf{R}_c) = \text{span}(\mathbf{C}) \approx \text{span}(\mathbf{U}_c) \tag{18}$$

where $\mathbf{U}_c \triangleq (\mathbf{u}_0 \ ; u_1 \ ; \cdots \ ; \mathbf{u}_{r_c-1})$. Note that although the functions $\{\psi_k(x)\}$ are orthogonal, the vectors $\{\mathbf{u}_k\}$ are in general not orthogonal. This is because of the fact that $\{\mathbf{u}_k\}$ are obtained by nonuniform sampling which destroys orthogonality. In practice, the PSWF $\psi_i(x)$ can be computed off-line and stored in the memory. When the parameters change, one can obtain the vectors $\mathbf{u}_k$ by resampling the PSWF $\psi_k(n+\gamma m+\beta l)$

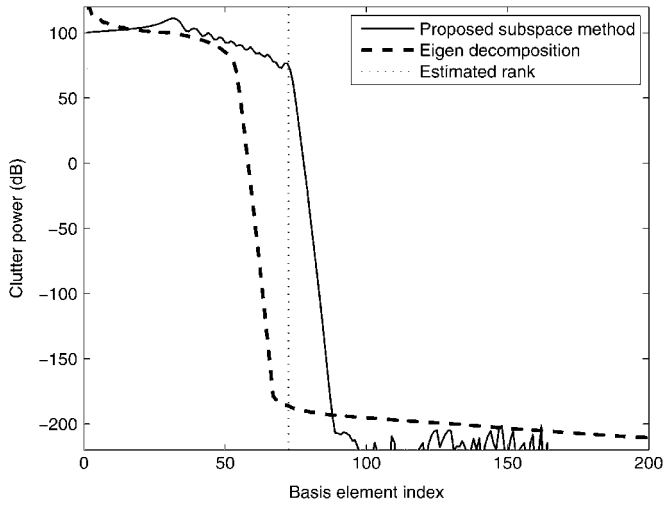

Fig. 6. Plot of the clutter power distributed in each of the orthogonal basis elements.

to form the new clutter subspace. In this way, we can obtain the clutter subspace by using the geometry of the problem.

Performing the Gram–Schmidt procedure on the basis $\{\mathbf{u}_k\}$, we obtain the orthonormal basis $\{\mathbf{q}_k\}$. The clutter power in each orthonormal basis element can be expressed as $\mathbf{q}_k^\dagger \mathbf{R}_c \mathbf{q}_k$. Fig. 6 shows the clutter power in the orthogonalized basis elements. In this example, $N = 10, M = 5, L = 16, \gamma = 10$, and $\beta = 1.5$. Note that there are a total of $NML = 800$ basis elements but we only show the first 200 on the plot. The clutter covariance matrix $\mathbf{R}_c$ is generated using the model described in [15]. The eigenvalues of $\mathbf{R}_c$ are also shown in Fig. 6 for comparison. The estimated clutter rank is $\lceil N + \gamma(M-1) + \beta(L-1) \rceil = 73$. One can see that the subspace obtained by the proposed method captures almost all clutter power. The clutter power decays to less than -200 dB for the basis index exceeding 90.

Compared to the eigendecomposition method, the subspace obtained by our method is larger. This is because of the fact that the clutter spatial bandwidth has been overestimated in this example. More specifically, we have assumed the worst case situation that the clutter spatial frequencies range from -0.5 to 0.5. In actual fact however, the range is only from -0.35 to 0.35. This comes about because of the specific geometry assumed in this example: the altitude is 9 km, the range of interest is 12.728 km, and a flat ground model is used. Therefore, the rank of the subspace is overestimated. It may seem that our method loses some efficiency compared to the eigendecomposition. However, note that the eigendecomposition requires perfect information of the clutter covariance matrix $\mathbf{R}_c$ while our method requires no data. In this example, we assume the perfect $\mathbf{R}_c$ is known. In practice, $\mathbf{R}_c$ has to be estimated from the received signals and it might not be accurate if the number of samples is not large enough. Note that, unlike the eigendecomposition method, the proposed method based on PSWF does not require the knowledge of $\mathbf{R}_c$.

V. New STAP Method for MIMO Radar

In this section, we introduce a new STAP method for MIMO radar which uses the clutter subspace estimation method described in the last section. Because the clutter subspace can be obtained by using the parameter information, the performance and complexity can both be improved. Recall that the optimal MVDR beamformer (11) requires knowledge of the covariance matrix $\mathbf{R}$. In practice, this has to be estimated from data. For example, it can be estimated as

$$\hat{\mathbf{R}} = \frac{1}{|\mathcal{B}|} \sum_{k \in \mathcal{B}} \mathbf{y}_k \mathbf{y}_k^\dagger \tag{19}$$

where $\mathbf{y}_k$ is the MIMO-STAP signal vector defined in (8) for the kth range bin, and $\mathcal{B}$ is a set which contains the neighbor range bin cells of the range bin of interest. However, some nearest cells around the range bin of interest are excluded from $\mathcal{B}$ in order to avoid including the target signals [32]. There are two advantages of using the target-free covariance matrix $\mathbf{R}$ in (11). First, it is more robust to steering vector mismatch. If there is mismatch in the steering vector $\mathbf{s}(f_s, f_D)$ in (9), the target signal is no longer protected by the constraint. Therefore, the target signal is suppressed as interference. This effect is called self-nulling, and it can be prevented by using a target-free covariance matrix. More discussion about self-nulling and robust beamforming can be found in [21] and [22] and the references therein. Second, using the target-free covariance matrix, the beamformer in (11) converges faster than the beamformer using the total covariance matrix. The famous rapid convergence theorem proposed by Reed *et al.* [25] states that a SINR loss of 3 dB can be obtained by using the number of target-free snapshots equal to twice the size of the covariance matrix. Note that the imprecise physical model which causes steering vector mismatch does not just create the self-nulling problem. It also affects the clutter subspace. Therefore, it affects the accuracy of the clutter subspace estimation in Section IV-B.

A. Proposed Method

The target-free covariance matrix can be expressed as $\mathbf{R} = \mathbf{R}_J + \mathbf{R}_c + \sigma^2 \mathbf{I}$, where $\mathbf{R}_J$ is the covariance matrix of the jammer signals, $\mathbf{R}_c$ is the covariance matrix of the clutter signals, and σ^2 is the variance of the white noise. By (18), there exists a $r_c \times r_c$ matrix $\mathbf{A}_c$ so that $\mathbf{R}_c \approx \mathbf{U}_c \mathbf{A}_c \mathbf{U}_c^\dagger$. Thus, the covariance matrix can be approximated by

$$\mathbf{R} \approx \underbrace{\mathbf{R}_J + \sigma^2 \mathbf{I}}_{\text{call this } \mathbf{R}_v} + \mathbf{U}_c \mathbf{A}_c \mathbf{U}_c^\dagger. \tag{20}$$

We assume the jammer signals $y_{n,m,l}^{(J)}$ in (6) are statistically independent in different pulses and different orthogonal waveform components [32]. Therefore, they satisfy

$$E[y_{n,m,l}^{(J)} \cdot y_{n',m',l'}^{(J)\dagger}] = \begin{cases} r_{J,n,n'}, & m = m', l = l' \\ 0, & \text{otherwise} \end{cases}$$

for $n, n' = 0, 1, \ldots, N, m, m' = 0, 1, \ldots, M$, and $l, l' = 0, 1, \ldots, L$. Using this fact, the jammer-plus-noise covariance matrix $\mathbf{R}_v$ defined in (20) can be expressed as

$$\mathbf{R}_v = \operatorname{diag}(\mathbf{R}_{vs}, \mathbf{R}_{vs}, \ldots, \mathbf{R}_{vs}) \tag{21}$$

where $\mathbf{R}_{vs}$ is an $N \times N$ matrix with elements $[\mathbf{R}_{vs}]_{n,n'} = r_{J,n,n'} + \sigma^2$ for $n, n' = 0, 1, \ldots, N$. Therefore, the covariance

matrix $\mathbf{R}$ in (20) consists of a *low-rank* clutter covariance matrix and a *block-diagonal* jammer-pulse-noise. By using the matrix inversion lemma [37], one can obtain

$$\mathbf{R}^{-1} \approx \mathbf{R}_v^{-1} - \mathbf{R}_v^{-1}\mathbf{U}_c(\mathbf{A}_c^{-1} + \mathbf{U}_c^\dagger \mathbf{R}_v^{-1}\mathbf{U}_c)^{-1}\mathbf{U}_c^\dagger \mathbf{R}_v^{-1}. \quad (22)$$

The inverse of the block-diagonal matrix $\mathbf{R}_v^{-1}$ is simply $\mathbf{R}_v^{-1} = \mathrm{diag}(\mathbf{R}_{vs}^{-1}, \mathbf{R}_{vs}^{-1}, \ldots, \mathbf{R}_{vs}^{-1})$, and the multiplication of the block-diagonal matrix with another matrix is simple.

B. Complexity of the New Method

The complexity of directly inverting the $NML \times NML$ covariance matrix $\mathbf{R}$ is $O(N^3M^3L^3)$. Taking advantage of the block-diagonal matrix and the low rank matrix, in (22), the complexity for computing $\mathbf{R}_v^{-1}$ is only $O(N^3)$ and the complexity for computing $\mathbf{A}_c^{-1}$ and $(\mathbf{A}_c + \mathbf{U}_c^\dagger \mathbf{R}_v^{-1}\mathbf{U}_c)^{-1}$ is only $O(r_c^3)$, where r_c is defined in (17). The overall complexity for computing (22) is thus reduced from $O(N^3M^3L^3)$ to $O(r_cN^2M^2L^2)$. This is the complexity of the multiplication of an $(NML \times r_c)$ matrix by an $(r_c \times NML)$ matrix.

C. Estimation of the Covariance Matrices

In (22), the matrix $\mathbf{U}_c$ can be obtained by the nonuniform sampling of the PSWF as described in the last section. The jammer-pulse-noise covariance matrix $\mathbf{R}_v$ and the matrix $\mathbf{A}_c$ both require further estimation from the received signals. Because of the block-diagonal structure, one can estimate the covariance matrix $\mathbf{R}_v$ by estimating its submatrix $\mathbf{R}_{vs}$ defined in (21). The matrix $\mathbf{R}_{vs}$ can be estimated when there are no clutter and target signals. For this, the radar transmitter *operates in passive mode* so that the receiver can collect the signals with only jammer signals and white noise [33]. The submatrix $\mathbf{R}_{vs}$ can be estimated as

$$\hat{\mathbf{R}}_{vs} = \frac{1}{K_v}\sum_{k=0}^{K_v-1} \mathbf{r}_k \mathbf{r}_k^\dagger \quad (23)$$

where $\mathbf{r}_k$ is an $N \times 1$ vector which represents the target-free and clutter-free signals received by N receiving antennas. By (20), one can express $\mathbf{A}_c$ as

$$\mathbf{A}_c = (\mathbf{U}_c^\dagger \mathbf{U}_c)^{-1}\mathbf{U}_c^\dagger(\mathbf{R} - \mathbf{R}_v)\mathbf{U}_c(\mathbf{U}_c^\dagger \mathbf{U}_c)^{-1}.$$

Therefore, one can estimate $\mathbf{A}_c$ by using

$$\hat{\mathbf{A}}_c = \frac{1}{K}\sum_{k=0}^{K-1} \mathbf{x}_k \mathbf{x}_k^\dagger - (\mathbf{U}_c^\dagger \mathbf{U}_c)^{-1}\mathbf{U}_c^\dagger \hat{\mathbf{R}}_v \mathbf{U}_c(\mathbf{U}_c^\dagger \mathbf{U}_c)^{-1} \quad (24)$$

where $\mathbf{x}_k = (\mathbf{U}_c^\dagger \mathbf{U}_c)^{-1}\mathbf{U}_c^\dagger \mathbf{y}_k$ and $\mathbf{y}_k$ is the $NML \times 1$ MIMO-STAP signal vector defined in (8). Substituting (23), (24) and (22) into the MIMO-STAP beamformer in (11), we obtain

$$\mathbf{w} \propto (\hat{\mathbf{R}}_v^{-1} - \hat{\mathbf{R}}_v^{-1}\mathbf{U}_c(\hat{\mathbf{A}}_c^{-1} + \mathbf{U}_c^\dagger \hat{\mathbf{R}}_v^{-1}\mathbf{U}_c)^{-1}\mathbf{U}_c^\dagger \hat{\mathbf{R}}_v^{-1})\mathbf{s}(f_s, f_d). \quad (25)$$

D. Zero-Forcing Method

Instead of estimating $\mathbf{A}_c$ and computing the MVDR by (25), one can directly "null out" the entire clutter subspace as described next. Assume that the clutter-to-noise ratio is very large and therefore all of the eigenvalues of $\mathbf{A}_c$ approach infinity. We obtain $\mathbf{A}_c^{-1} \approx \mathbf{0}$. Substituting it into (25), one can obtain the MIMO-STAP beamformer as

$$\mathbf{w} \propto (\hat{\mathbf{R}}_v^{-1} - \hat{\mathbf{R}}_v^{-1}\mathbf{U}_c(\mathbf{U}_c^\dagger \hat{\mathbf{R}}_v^{-1}\mathbf{U}_c)^{-1}\mathbf{U}_c^\dagger \hat{\mathbf{R}}_v^{-1})\mathbf{s}(f_s, f_d). \quad (26)$$

Thus we obtain a "zero-forcing" beamformer that nulls out the entire clutter subspace. The advantage of this zero-forcing method is that it is no longer necessary to estimate $\mathbf{A}_c$. In this method, we only need to estimate $\mathbf{R}_{vs}$. The method is independent of the range bin. The matrix $\mathbf{R}^{-1}$ computed by this method can be used for all range bins. Because there are lots of extra dimensions in MIMO radars, dropping the entire clutter subspace will reduce only a small portion of the total dimension. Therefore, it will not affect the SINR performance significantly, as we shall demonstrate. Thus, this method can be very effective in MIMO radars.

E. Comparison With Other Methods

In the sample matrix inversion (SMI) method [32], the covariance matrix is estimated to be the quantity $\hat{\mathbf{R}}$ in (19) and $\hat{\mathbf{R}}^{-1}$ is directly used in (11) to obtain the MVDR beamformer. However, some important information about the covariance matrix is unused in the SMI method. This information includes the parameters γ and β, the structure of the clutter covariance matrix, and the block-diagonal structure of the jammer covariance matrix.

Our method in (25) utilizes this information. We first estimate the clutter subspace by using parameters γ and β in (18). Because the jammer matrix is block diagonal and the clutter matrix has low rank with known subspace, by using the matrix inversion lemma, we could break the inversion of a large matrix $\mathbf{R}$ into the inversions of some smaller matrices. Therefore, the computational complexity was significantly reduced. Moreover, by using the structure, fewer parameters need to be estimated. In our method, only the $r_c \times r_c$ matrix $\mathbf{A}$ and the $N \times N$ matrix $\mathbf{R}_{vs}$ need to be estimated rather than the $NML \times NML$ matrix $\mathbf{R}$ in the SMI method. Therefore, our method also converges much faster.

In subspace methods [27]–[33], the clutter and the jammer subspace are both estimated simultaneously using the STAP signals rather than from problem geometry. Therefore, the parameters γ and β and the block-diagonal structure of the jammer covariance matrix are not fully utilized. In [26], the target-free and clutter-free covariance matrix are also estimated using (23). The jammer and clutter are filtered out in two separate stages. Therefore, the block-diagonal property of the jammer covariance matrix has been used in [26]. However, the clutter subspace structure has not been fully utilized in this method.

VI. Numerical Examples

In this section, we compare the SINR performance of our methods and other existing methods. In the example, the pa-

rameters are $M = 5, N = 10, L = 16, \beta = 1.5$ and $\gamma = 10$. The altitude is 9 km, and the range of interest is 12.728 km. For this altitude and range, the clutter is generated by using the model in [15]. The clutter-to-noise ratio (CNR) is 40 dB. There are two jammers at 20° and $-30°$. The jammer-to-noise ratio (JNR) for each jammer equals 50 dB. The SINR is normalized so that the maximum SINR equals 0 dB. The jammers are modelled as point sources which emit independent white Gaussian signals. The clutter is modeled using discrete points as described in (2). The clutter points are equally spaced on the range bin and the RCS for each clutter is modelled as identical independent Gaussian random variables. In general, the variance of ρ_i will vary along the ground, as we move within one range bin. However, for simplicity we assume this variance is fixed. The number of clutter points N_c is 10 000. The clutter points for different range bins are also independent. The following methods are compared.

1) *Sample matrix inversion (SMI) method* [32]: This method estimates the covariance matrix $\mathbf{R}$ using (9) and directly substitutes it into (11).
2) *Loaded sample matrix inversion (LSMI) method* [23], [24]: Before substituting $\hat{\mathbf{R}}$ into (11), a diagonal loading $\hat{\mathbf{R}} \leftarrow \hat{\mathbf{R}} + \delta\mathbf{I}$ is performed. In this example, δ is chosen as ten times the white noise level.
3) *Principal component (PC) method* [32]: This method uses a KLT filterbank to extract the jammer-plus-clutter subspace. Then the space–time beamforming can be performed in this subspace.
4) *Separate jammer and clutter cancellation method* [26] (abbreviated as SJCC below): This method also utilizes the jammer-plus-noise covariance matrix $\mathbf{R}_{vs}$, which can be estimated as in (23). The covariance matrix can be used to filter out the jammer and form a spatial beam. Then, the clutter can be further filtered out by space–time filtering [26]. In this example, a diagonal loading is used for the space–time filtering with a loading factor, which equals ten times the white noise level.
5) *The new zero-forcing (ZF) method*: This method directly nulls out the clutter subspace as described in (26).
6) *The new minimum variance method*: This method estimates $\hat{\mathbf{R}}_{vs}$ and $\hat{\mathbf{A}}_c$ and uses (25). In this example, a diagonal loading is used for $\hat{\mathbf{A}}_c$ with a loading factor that equals ten times the white noise level.
7) *MVDR with perfectly known* $\mathbf{R}$: This method is unrealizable because the perfect $\mathbf{R}$ is always unavailable. It is shown in the figure because it serves as an upper bound on the SINR performance.

Fig. 7 shows the comparison of the SINR for $f_s = 0$ as a function of the Doppler frequencies. The SINR is defined as

$$\text{SINR} \triangleq \frac{|\mathbf{w}^\dagger \mathbf{s}(f_s, f_D)|^2}{\mathbf{w}^\dagger \mathbf{R} \mathbf{w}}$$

where $\mathbf{R}$ is the target-free covariance matrix. To compare these methods, we fix the number of samples K and the number of jammer-plus-noise samples K_v. In all of the methods except the SMI method, 300 samples and 20 jammer-plus-noise samples are used. We use 2000 samples instead of 300 samples in the SMI method because the estimated covariance matrix in (19) with 300 samples is not full-rank and therefore cannot be inverted. The spatial beampatterns and space–time beampatterns for the target at $f_s = 0$ and $f_D = 0.25$ for four of these methods are shown in Figs. 8 and 9, respectively. The spatial beampattern is defined as

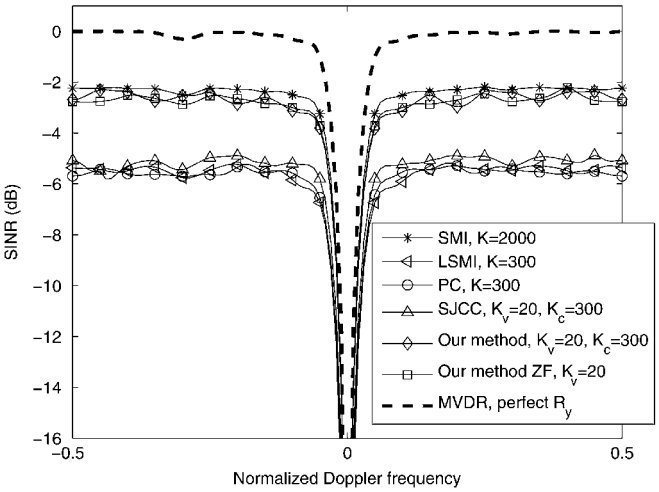

Fig. 7. SINR performance of different STAP methods at looking direction zero as a function of the Doppler frequency.

$$\sum_{k=0}^{ML-1} |\mathbf{w}^\dagger_{(1:N)+kML} \mathbf{s}(f_s)|^2$$

where $\mathbf{s}(f_s)$ is the spatial steering vector

$$(1 e^{j2\pi f_s} \cdots e^{j2\pi f_s (N-1)})^T$$

and $\mathbf{w}_{(1:N)+kML}$ represents N successive elements of $\mathbf{w}$ starting from $kML+1$. The space–time beampattern is defined as

$$|\mathbf{w}^\dagger \mathbf{s}(f_s, f_D)|$$

where $\mathbf{s}(f_s, f_D)$ is the space–time steering vector defined in (10). The spatial beampattern represents the jammer and noise rejection and the space–time beampattern represents the clutter rejection. In Fig. 8, one can see the jammer notches at the corresponding jammer arrival angles $-30°$ and 20°. In Fig. 9, one can also observe the clutter notch in the beampatterns. In Fig. 7, lacking use of the covariance matrix structure, the SMI method requires a lot of samples to obtain good performance. It uses 2000 samples, but the proposed minimum variance method, which has a comparable performance, uses only 300 samples. The PC method and LSMI method utilize the fact that the jammer-plus-clutter covariance matrix has low rank. Therefore, they require fewer samples than the SMI method. The performance of these two are about the same. The SJCC method further utilizes the fact that the jammer covariance matrix is block diagonal and estimates the jammer-plus-noise covariance matrix. Therefore, the SINR performance is slightly

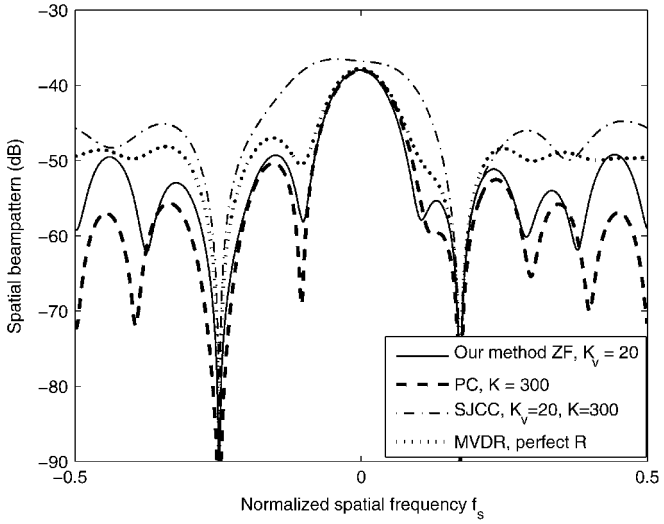

Fig. 8. Spatial beampatterns for four STAP methods.

better than the LSMI and PC methods. Our methods not only utilize the low rank property and the block-diagonal property but also the geometry of the problem. Therefore, our methods have better SINR performance than the SJCC method. The proposed ZF method has about the same performance as the minimum variance method. It converges to a satisfactory SINR with very few clutter-free samples. According to (16), the clutter rank in this example is approximately

$$\lceil N + \gamma(M-1) + \beta(L-1) \rceil = 73.$$

Thanks to the MIMO radar, the dimension of the space–time steering vector is $MNL = 800$. The clutter rank is just a small portion of the total dimension. This is the reason why the ZF method, which directly nulls out the entire clutter space, works so well.

VII. Conclusion

In this paper, we first studied the clutter subspace and its rank in MIMO radars using the geometry of the system. We derived an extension of Brennan's rule for estimating the dimension of the clutter subspace in MIMO radar systems. This rule is given in (16). An algorithm for computing the clutter subspace using nonuniform sampled PSWF was described. Then, we proposed a space–time adaptive processing method in MIMO radars. This method utilizes the knowledge of the geometry of the problem, the structure of the clutter space, and the block-diagonal structure of the jammer covariance matrix. Using the fact that the jammer matrix is block diagonal and the clutter matrix has low rank with known subspace, we showed how to break the inversion of a large matrix $\mathbf{R}$ into the inversions of smaller matrices using the matrix inversion lemma. Therefore, the new method has much lower computational complexity. Moreover, we can directly null out the entire clutter space for large clutter. In our ZF method, only the $N \times N$ jammer-plus-noise matrix $\mathbf{R}_{vs}$ needs to be estimated instead of the $NML \times NML$ matrix $\mathbf{R}$ in the SMI method, where N is the number of receiving antennas, M is the number of transmitting antennas, and L is the number of pulses in a coherent processing interval. Therefore, for a given number of data samples, the new method has better

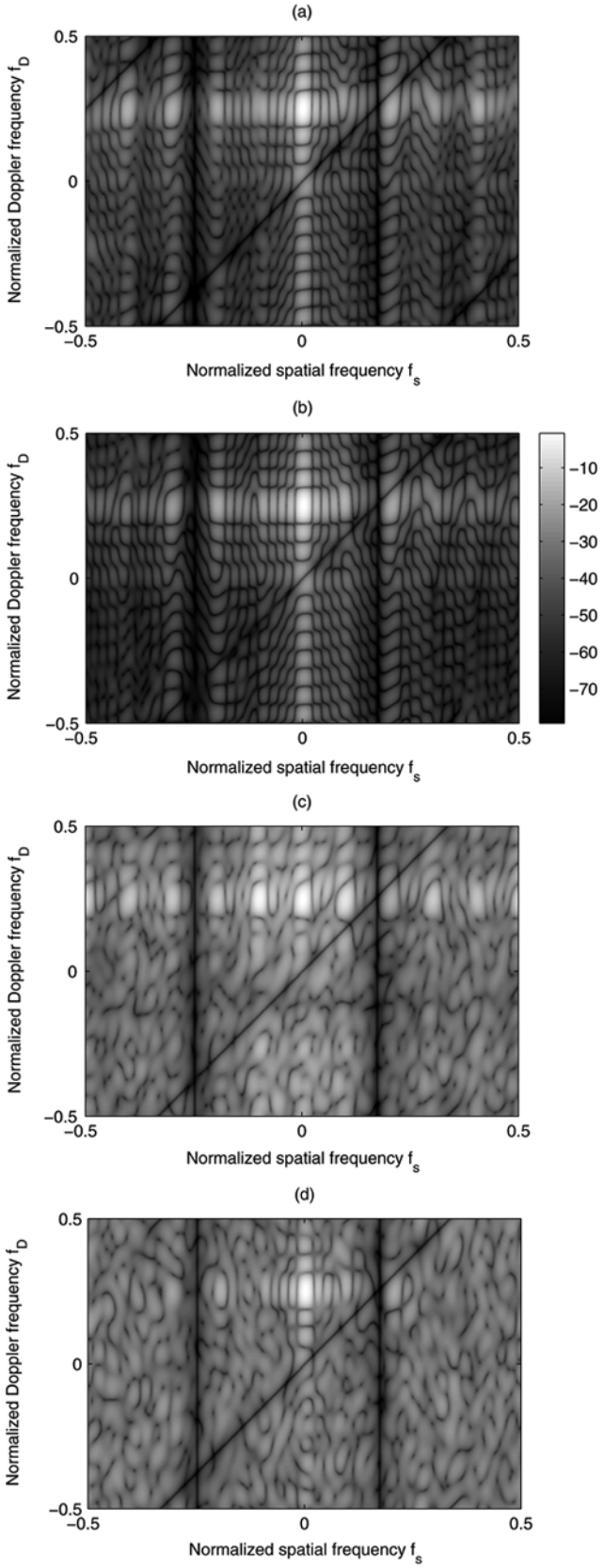

Fig. 9. Space–time beampatterns for four methods: (a) Proposed zero-forcing method; (b) principal component (PC) method [32]; (c) separate jammer and clutter cancellation method (SJCC) [26]; and (d) SMI method [32].

performance. In Section VI, we provided an example where the number of training samples was reduced by a factor of 100 with no appreciable loss in performance compared to the SMI method.

In practice, the clutter subspace might change because of effects such as the ICM, velocity misalignment, array manifold mismatch, and channel mismatch [32]. In this paper, we considered an "ideal model," which does not take these effects into account. When this model is not valid, the performance of the algorithm will degrade. One way to overcome this might be to estimate the clutter subspace by using a combination of both the assumed geometry and the received data. Another way might be to develop a more robust algorithm against the clutter subspace mismatch. These ideas will be explored in the future.

REFERENCES

[1] D. J. Rabideau and P. Parker, "Ubiquitous MIMO multifunction digital array radar," in *Proc. 37th IEEE Asilomar Conf. Signals, Systems, Computers*, Nov. 2003, vol. 1, pp. 1057–1064.

[2] D. W. Bliss and K. W. Forsythe, "Multiple-input multiple-output (MIMO) radar and imaging: Degrees of freedom and resolution," in *Proc. 37th IEEE Asilomar Conf. Signals, Systems, Computers*, Nov. 2003, vol. 1, pp. 54–59.

[3] E. Fishler, A. Haimovich, R. S. Blum, D. Chizhik, L. J. Cimini, and R. A. Valenzuela, "MIMO Radar: An idea whose time has come," in *Proc. IEEE Radar Conf.*, Apr. 2004, pp. 71–78.

[4] E. Fishler, A. Haimovich, R. S. Blum, L. J. Cimini, D. Chizhik, and R. A. Valenzuela, "Performance of MIMO radar systems: Advantages of angular diversity," in *Proc. 38th IEEE Asilomar Conf. Signals, Systems, Computers*, Nov. 2004, vol. 1, pp. 305–309.

[5] E. Fishler, A. Haimovich, R. S. Blum, L. J. Cimini, D. Chizhik, and R. A. Valenzuela, "Spatial diversity in radars—models and detection performance," *IEEE Trans. Signal Process.*, vol. 54, no. 3, pp. 823–837, Mar. 2007.

[6] F. C. Robey, S. Coutts, D. Weikle, J. C. McHarg, and K. Cuomo, "MIMO radar theory and experimental results," in *Proc. 38th IEEE Asilomar Conf. Signals, Systems, Computers*, Nov. 2004, vol. 1, pp. 300–304.

[7] K. W. Forsythe, D. W. Bliss, and G. S. Fawcett, "Multiple-input multiple-output (MIMO) radar performance issues," in *Proc. 38th IEEE Asilomar Conf. Signals, Systems, Computers*, Nov. 2004, pp. 310–315.

[8] H. A. Khan, W. Q. Malik, D. J. Edwards, and C. J. Stevens, "Ultra wideband multiple-input multiple-output radar," in *Proc. IEEE Int. Radar Conf.*, May 2005, pp. 900–904.

[9] H. A. Khan and D. J. Edwards, "Doppler problems in orthogonal MIMO radars," in *Proc. IEEE Int. Radar Conf.*, Apr. 2007, pp. 24–27.

[10] V. F. Mecca, D. Ramakrishnan, and J. L. Krolik, "MIMO radar space–time adaptive processing for multipath clutter mitigation," *Proc. IEEE Workshop Sensor Array Multichannel Signal Processing*, pp. 249–253, Jul. 2007.

[11] D. R. Fuhrmann and G. S. Antonio, "Transmit beamforming for MIMO radar systems using partial signal correlation," in *Proc. 38th IEEE Asilomar Conf. Signals, Systems, Computers*, Nov. 2004, pp. 295–299.

[12] G. S. Antonio and D. R. Fuhrmann, "Beampattern synthesis for wideband MIMO radar systems," *Proc. 1st IEEE Int. Workshop Computational Advances in Multi-Sensor Adaptive Processing*, pp. 105–108, Dec. 2005.

[13] K. W. Forsythe and D. W. Bliss, "Waveform correlation and optimization issues for MIMO radar," in *Proc. 39th IEEE Asilomar Conf. Signals, Systems, Computers*, Nov. 2005, pp. 1306–1310.

[14] Q. Zhang and W. B. Mikhael, "Estimation of the clutter rank in the case of subarraying for space–time adaptive processing," *Electron. Lett.*, vol. 33, no. 5, pp. 419–420, Feb. 27, 1997.

[15] N. A. Goodman and J. M. Stiles, "On clutter rank observed by arbitrary arrays," *IEEE Trans. Signal Process.*, vol. 55, no. 1, pp. 178–186, Jan. 2007.

[16] J. Ward, "Space–time adaptive processing for airborne radar," Lincoln Laboratory, Lexington, MA, Tech. Rep. 1015, Dec. 1994.

[17] L. E. Brennan and F. M. Staudaher, "Subclutter visibility demonstration," Adeptive Sensors, Inc., Santa Monica, CA, Tech. Rep. RL-TR-92-21, 1992.

[18] R. Klemm, "Adaptive clutter suppression for airborne phased array radars," *Proc. Inst. Elect. Eng. F*, vol. 130, no. 1, pp. 125–132, 1983.

[19] D. Slepian and H. O. Pollak, "Prolate spheroidal wave functions, Fourier analysis and uncertainty—III: The dimension of the space of essentially time-and-band-limited signals," *Bell Syst. Tech. J.*, pp. 1295–1336, Jul. 1962.

[20] J. Capon, "High-resolution frequency-wavenumber spectrum analysis," *Proc. IEEE*, vol. 57, no. 8, pp. 1408–1418, Aug. 1969.

[21] C. Y. Chen and P. P. Vaidyanathan, "Quadratically constrained beamforming robust against direction-of-arrival mismatch," *IEEE Trans. Signal Process.*, accepted for publication.

[22] R. G. Lorenz and S. P. Boyd, "Robust minimum variance beamforming," *IEEE Trans. Signal Process.*, vol. 53, no. 5, pp. 1684–1696, May 2005.

[23] Y. I. Abramovich, "Controlled method for adaptive optimization of filters using the criterion of maximum SNR," *Radio Eng. Electron. Phys.*, vol. 26, pp. 87–95, Mar. 1981.

[24] B. D. Carlson, "Covariance matrix estimation errors and diagonal loading in adaptive arrays," *IEEE Trans. Aerosp. Electron. Syst.*, vol. 24, no. 4, pp. 397–401, Jul. 1988.

[25] J. S. Reed, J. D. Mallett, and L. E. Brennan, "Rapid convergence rate in adaptive arrays," *IEEE Trans. Aerosp. Electron. Syst.*, vol. AES-10, no. 6, pp. 853–863, Nov. 1974.

[26] R. Klemm, "Adaptive air- and spaceborne MTI under jamming conditions," in *Proc. IEEE Nat. Radar Conf.*, Apr. 1993, pp. 167–172.

[27] J. R. Guerci, J. S. Goldstein, and I. S. Reed, "Optimal and adaptive reduced-rank STAP," *IEEE Trans. Aerosp. Electron. Syst. (Special Section on Space–Time Adaptive Processing)*, vol. 36, no. 2, pp. 647–663, Apr. 2000.

[28] A. M. Haimovich and M. Berin, "Eigenanalysis-based space–time adaptive radar: performance analysis," *IEEE Trans. Aerosp. Electron. Syst.*, vol. 33, no. 4, pp. 1170–1179, Oct. 1997.

[29] J. S. Goldstein, I. Si. Reed, and L. L. Scharf, "A multistage representation of the Wiener filter based on orthogonal projections," *IEEE Trans. Inf. Theory*, vol. 44, no. 7, pp. 2943–2959, Nov. 1998.

[30] B. Friedlander, "A subspace method for space time adaptive processing," *IEEE Trans. Signal Process.*, vol. 53, no. 1, pp. 74–82, Jan. 2005.

[31] X. Wen, A. Wang, L. Li, and C. Han, "Direct data domain approach to space–time adaptive signal processing," *Proc. Int. Conf. Control, Automation, Robotics, Vision (ICARCV)*, vol. 3, pp. 2070–2075, Dec. 2004.

[32] J. R. Guerci, *Space–Time Adaptive Processing*. Norwood, MA: Artech House, 2003.

[33] R. Klemm, *Principles of Space–Time Adaptive Processing*. London, U.K.: IEE, 2002.

[34] M. A. Richards, *Fundamentals of Radar Signal Processing*. New York: McGraw-Hill, 2005.

[35] H. L. Van Trees, *Optimum Array Processing: Part IV of Detection Estimation and Modulation Theory*. New York: Wiley Interscience, 2002.

[36] J. P. Keener, *Principles of Applied Mathematics*. Reading, MA: Addison-Welsley, 1988.

[37] R. A. Horn and C. R. Johnson, *Matrix Analysis*. Cambridge, U.K.: Cambridge Univ. Press, 1985.

Chun-Yang Chen (S'06) was born in Taipei, Taiwan, R.O.C., on November 22, 1977. He received the B.S. and M.S. degrees in electrical engineering and communication engineering, both from National Taiwan University (NTU), Taipei, Taiwan, R.O.C., in 2000 and 2002, respectively. He is currently working towards the Ph.D. degree in electrical engineering in the field of digital signal processing at California Institute of Technology (Caltech), Pasadena.

His interests currently include signal processing in MIMO communications, ultra-wideband communications, and radar applications.

P. P. Vaidyanathan (S'80–M'83–SM'88–F'91) was born in Calcutta, India, on October 16, 1954. He received the B.Sc. (Hons.) degree in physics and the B.Tech. and M.Tech. degrees in radiophysics and electronics, all from the University of Calcutta, India, in 1974, 1977, and 1979, respectively, and the Ph.D. degree in electrical and computer engineering from the University of California at Santa Barbara in 1982.

He was a Postdoctoral Fellow at the University of California, Santa Barbara, from September 1982 to March 1983. In March 1983, he joined the Electrical Engineering Department of the California Institute of Technology, Pasadena, as an Assistant Professor, where he has been a Professor of electrical engineering since 1993. His main research interests are in digital signal processing, multirate systems, wavelet transforms, and signal processing for digital communications. He has authored a number of papers in IEEE journals and is the author of the book *Multirate Systems and Filter Banks* (Englewood Cliffs, NJ: Prentice-Hall, 1993). He has written several chapters for various signal processing handbooks.

Dr. Vaidyanathan served as Vice-Chairman of the Technical Program Committee for the 1983 IEEE International Symposium on Circuits and Systems, and as the Technical Program Chairman for the 1992 IEEE International Symposium on Circuits and Systems. He was an Associate Editor for the IEEE TRANSACTIONS ON CIRCUITS AND SYSTEMS for the period 1985 to 1987, and is currently an Associate Editor for the IEEE SIGNAL PROCESSING LETTERS and a Consulting Editor for the journal *Applied and Computational Harmonic Analysis*. He was a Guest Editor in 1998 for special issues of the IEEE TRANSACTIONS ON SIGNAL PROCESSING and the IEEE TRANSACTIONS ON CIRCUITS AND SYSTEMS II, on the topics of filter banks, wavelets, and subband coders. He was a recipient of the Award for Excellence in Teaching at the California Institute of Technology for the years 1983–1984, 1992–1993, and 1993–1994. He also received the NSF's Presidential Young Investigator Award in 1986. In 1989, he received the IEEE Acoustics, Speech and Signal Processing (ASSP) Senior Award for his paper on multirate perfect-reconstruction filter banks. In 1990, he was recipient of the S. K. Mitra Memorial Award from the Institute of Electronics and Telecommunications Engineers, India, for his joint paper in the *Institution of Electronics and Telecommunication Engineers* (IETE) journal. He was also the coauthor of a paper on linear-phase perfect reconstruction filter banks in the IEEE TRANSACTIONS ON SIGNAL PROCESSING, for which the first author (T. Nguyen) received the Young Outstanding Author Award in 1993. He received the 1995 F. E. Terman Award of the American Society for Engineering Education, sponsored by Hewlett-Packard Company, for his contributions to engineering education, especially for the book *Multirate Systems and Filter Banks*. He has given several plenary talks, at such conferences on signal processing as SAMPTA'01, EUSIPCO'98, SPCOM'95, and Asilomar'88. He has been chosen a Distinguished Lecturer for the IEEE Signal Processing Society for the year 1996–1997. In 1999, he was chosen to receive the IEEE Circuits and System Society's Golden Jubilee Medal. He is a recipient of the IEEE Signal Processing Society's Technical Achievement Award for the year 2002.